

# Molecular Dynamics of a Fluid

## Confined in Kerosen from Memory Kernels

Kristina Ariskina<sup>†</sup>, Guillaume Galliéro<sup>‡</sup>, Amaël Obliger<sup>‡</sup>

<sup>†</sup>Laboratoire des Fluides Complexes et leurs Réservoirs, Univ. of Pau and Pays de l'Adour/CNRS/TotalEnergies/E2S, UMR 5150 Pau 64000, France

<sup>‡</sup>Institut des Sciences Moléculaires, Univ. of Bordeaux, CNRS, UMR 5255, Talence 33405, France

### RESEARCH MOTIVATION

The profound knowledge of solid-fluid couplings is crucial in the framework of shale gas extraction characterized by an extreme production decline rate. The inherent flexibility of all organic matter or kerosen plays an important role on the dynamics of fluid releases from the solid matrix (Fig. 1). The fairly promising technique based on the iterative reconstruction of, so called, memory kernel proposed in this work allows directly estimate the impact of the solid (kerosen) on fluid dynamics at the mesoscale.

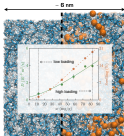


Fig. 1. Adsorption induced swelling effect on transport. The diffusion coefficient ( $D = D_0$ ) and swelling versus CH<sub>4</sub> loading for 400 K, 25 MPa within flexible kerosen shown in the background. Trajectory length is  $\sim 100$  ns with 10 fs per processing resolution

### PURPOSES

- investigating small and intermediate time couplings between the dynamics of the solid and the fluid
- understanding the flexibility effects from the comparison between the flexible and rigidified kerosen molecular models
- assessing the prediction of transport properties from the atomic velocity/force and memory kernel

### GENERALIZED LANGEVIN FRAMEWORK

The generalized Langevin equation allows to extract memory kernel  $K$  from a coarse-grained fluid particle dynamics affected by the friction force (first term) and the noise  $\eta$  (second term) (Eq. 1):

$$m \frac{du}{dt} = - \int_0^t K(u)v(t-u)du + \eta(t) \quad (1) \quad K = \frac{1}{k_B T} \langle \eta(t)\eta(0) \rangle \quad (2)$$

$K$  and  $\eta$  are coupled through the fluctuation-dissipation theorem (Eq. 2) [2].

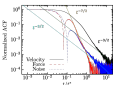


Fig. 2. Normalized velocity (VACF), force (FACF) and noise (NACF) auto-correlation functions as the functions of time in Lennard-Jones LJ units.  $t^*$  is the LJ time for CH<sub>4</sub> (1.246 ps)

First, we reproduced recent results of D. Lesnicki on the monoatomic fluid hydrodynamics [3] (Fig. 2). The VACF follows the scaling  $\sim t^{-3/2}$  at long times attributed to hydrodynamic modes. The memory kernel (NACF) reconstructed by inverting the Volterra equation of the second kind [3] decays the same way as the VACF.

### LOADING EFFECT ON CORRELATION FUNCTIONS

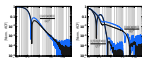


Fig. 3. The velocity (left), force and noise (right) normalized ACFs for flexible kerosen with low (blue curve) and high (black curve) CH<sub>4</sub> loading. The FACF is not shown after 10 ps to large space on the graph

The characteristic peak in the VACF in the case of flexible kerosen (Fig. 3) indicates strong fluid confinement compared to that for a bulk fluid (Fig. 2). Furthermore, the memory kernel decays much slower than the VACF and the FACF signifying important memory effects.

### FLEXIBILITY EFFECT ON CORRELATION FUNCTIONS

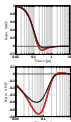


Fig. 4. The normalized ACFs for flexible (black line) and rigidified kerosen with high CH<sub>4</sub> content. The curves of other than black colors show 5 different configurations rigidified. 5 slices of 20 ns for each run are used for the error bars

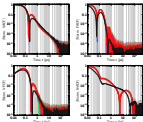


Fig. 5. Absolute values of the normalized ACFs for flexible (black line) and rigidified kerosen with high CH<sub>4</sub> loading. The curves of other than black colors show 5 different configurations rigidified

The different rigidified configurations show similar behaviour (Fig. 4). The kerosen matrix rigidification causes the pronounced rattling effect as it can be seen on the negative peak of the ACFs (Fig. 5).

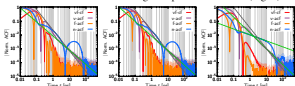


Fig. 6. The normalized ACFs for the rigidified configurations showing the slowest (left) and fastest (middle) diffusion rates and for the flexible (right) configuration with high CH<sub>4</sub> content

The VACF follows a  $t^{-1}$  scaling in the rigidified case (Fig. 6) instead of the generic  $t^{-3/2}$  scaling that corresponds to both hydrodynamics and Rouse polymer diffusion. The VACF scaling for flexible kerosen lies between the above-mentioned scalings. Memory kernel as another ACFs do not follow the hydrodynamic modes for a fluid confined in the kerosen matrix.

### TRANSPORT COEFFICIENT ESTIMATION

The diffusion coefficient is computed from the integrals of memory kernel, the FACF (Eq. 3) and the VACF (Eq. 4):

$$D(t) = \frac{k_B T}{\xi(t)} \begin{cases} \xi(t) = \frac{1}{k_B T} \int_0^t \langle f(s)f(0) \rangle ds \\ \xi(t) = \int_0^t \langle K(s) \rangle ds \end{cases} \quad (3) \quad D(t) = \frac{1}{6} \int_0^t \langle v(s)v(0) \rangle ds \quad (4)$$

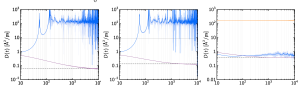


Fig. 7. The  $D$  obtained from the integrals of the VACF (blue curve), VACF (violet curve) and memory kernel (orange curve) for the rigidified configurations showing the slowest (left) and fastest (middle) diffusion rates and for the flexible (right)

Memory kernel reproduces well the  $D$  from the VACF compared to the FACF for flexible kerosen (Fig. 7) while for its rigidified model diffusion mechanism can not be revealed.

### REFERENCES

- [1] A. Obliger et al., Journal of Physical Chemistry B, 123(26):5635–5640, 2019.
- [2] G. Jung et al., Journal of Chemical Theory and Computation, 13(6): 2481–2488, 2017.
- [3] D. Lesnicki et al., Physical Review Letters, 116(4): 1–5, 2016.